SPIRAL VORTICES DETECTION ON A ROTATING DISK

T. Astarita, G. Cardone and G.M. Carlomagno
University of Naples - DETEC
P.le Tecchio, 80 - 80125 Naples, ITALY

Keywords: *Spiral vortices, Rotating disk, IR thermography*

Abstract

The spiral vortices that arise in the transitional regime of the three-dimensional boundary layer on a rotating disk are experimentally investigated by means of Infrared (IR) Thermography.

In order to detect the spiral vortices, which rotate attached to the disk surface, this latter one is uniformly heated with a printed circuit board and the line scan facility of the infrared system is used.

A reconstruction of the thermal image, joined with an application software, allows for counting the number of vortices and their inclination as a function of the local Reynolds number.

1 Introduction

The characteristics of the flow field and of the distribution of the convective heat transfer coefficient in rotating system are both practically and theoretically relevant.

Rotating elements are widely used in many practical applications and even if the fluid resistance is, in most cases, irrelevant the thermal analysis is of utmost importance. Of all the possible real geometrical shapes, probably the rotating disk is the simplest one and many geometrical configurations may be practically represented in terms of a rotating disk. Really the flywheels, the disk brakes, the disks to which the turbine blades are attached and even the modern high speed CD-ROM are all examples of practical application of this type of flow.

From a strictly engineering point of view, the parameters that interest the designer are essentially the stress level, due to both mechanical and thermal loads as well as the fatigue life of the component. However, these parameters may be only evaluated on the basis of a detailed knowledge of the local temperature distribution, and therefore of the heat transfer coefficient, for different operating conditions.

For its evident practical applications, the distribution of the convective heat transfer coefficient both in the laminar and turbulent regime has been extensively studied in the past; e.g. the papers by Millsaps and Pohlhausen [1], Cobb and Saunders [2], Northrop and Owen [3] and Astarita et al. [4] are herein recalled.

The presence of both the centrifugal and Coriolis force normally plays a significant part in the development of the laminar flow field on a rotating disk complicating the theoretical analysis. The fore mentioned forces also, seriously affect the study of the stability and of the transition to turbulence. In many practical application, the formation of stable vortex patterns is well known.

The existence of an exact solution (Kàrmàn, 1921[5]) of the laminar velocity field on a rotating disk combined to the three-dimensional nature of the flow field has produced a great interest in the theoretical study of the transitional regime. In particular, the works by Kohama and co-workers [6], [7] and by Malik and co-workers [8], [9] are acknowledged. Both these research groups approached the problem both theoretically and experimentally.

The main results of the theoretical analysis of Kohama and co-workers were that the angle j, which the spiral vortex makes with respect to the direction normal to the local radius, should

be practically constant and equal to 14°; besides, they initially claimed that a phase velocity between the spiral vortices and the rotating disk existed. Furthermore, they found that the vortices co-rotate all in the same direction. The experimental results of the same research group, carried on by means of flow visualisations and hot wire measurements, however, showed that the angle j is confined in the interval 5° to 15° and that the expected phase velocity is, actually, zero, i.e., the spiral vortices are stationary with respect to the rotating disk. The number of vortices is said to vary in the interval 30 to 34 independently of the angular velocity of the disk.

Also the theoretical analysis of Malik and co-workers showed that the angle j should be practically constant but they found it equal to 11.2°. The number of vortices N should linearly increase with the square root of the local Reynolds number Re_r:

$$N = 0.0698 \sqrt{Re_r} \qquad (1)$$

Their experimental results, also carried out by means of hot wire measurements, confirmed the general trend of equation (1) even if the experimental data fall well below the theoretical curve at high Reynolds numbers.

The purpose of this work is to perform flow visualizations of the spiral vortices on a rotating disk in still air by means of infrared thermography. The vortex visualizations are also elaborated in order to measure both the angle j and the number of vortices on the disk.

2 Experimental apparatus and procedure

A sketch of the experimental apparatus is shown in Fig. 1. The disk section consists of a $450mm$ diameter steel cup, filled with a $20mm$ thick polystyrene foam slab on which a printed circuit board is glued. The circuit is used to generate, by Joule effect, a uniform heat flux at the disk surface, whereas the foam thermally insulates the face of the disk not exposed to ambient air.

The printed circuit board is designed so as to achieve a constant heat flux over the disk surface and therefore the thickness and width of its conducting tracks are realized with very close tolerances. The tracks, having a double spiral shape, are $35mm$ thick, $1.8mm$ wide and placed at $2mm$ steps; the overall thickness of the board is $0.3mm$.

In order to enhance the detection of the emitted IR radiation, the measured board surface is coated with a thin layer of black paint which has an emissivity coefficient equal to 0.95 in the working IR band of the employed scanner.

Electric power is supplied to the printed circuit by means of a mercury rotating contact.

A pulley, which is connected by a transmission belt to an electric motor, is fixed on the shaft supporting the disk. By changing the pulley and/or varying the electrical frequency, it is possible to vary the rotational speed of the disk in a continuos way within the range 100-2000rpm.

The thermographic system is also used to monitor the rotational speed of the disk. In fact for each test, an optical transducer emits an electrical signal for each disk rotation and an acquisition board (1MHz) of the thermographic
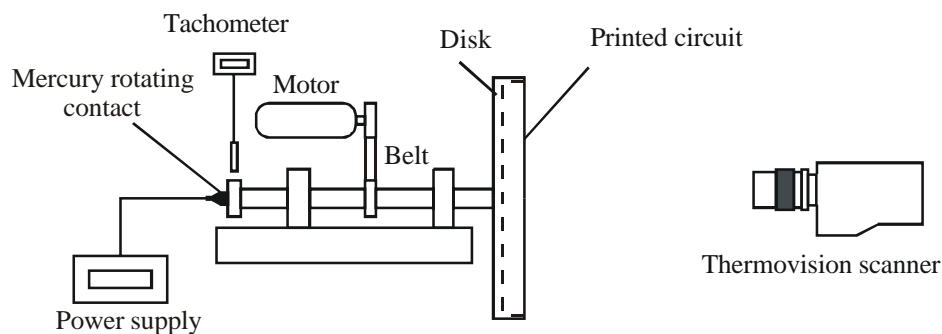

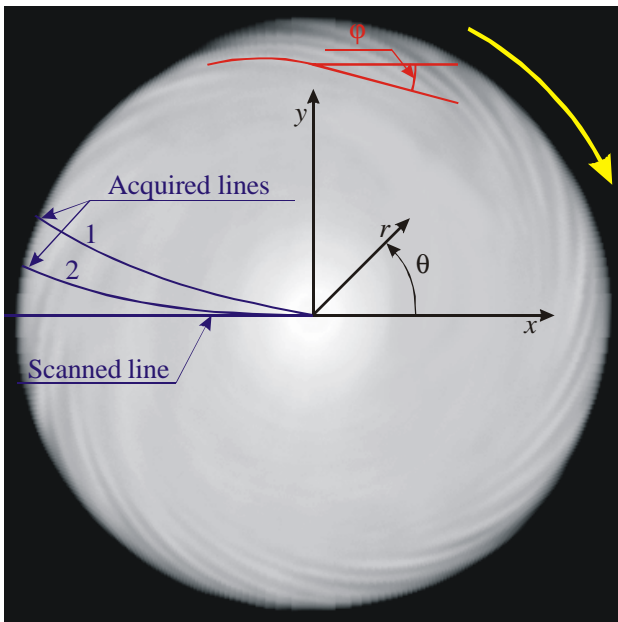Fig. 1 – Sketch of the experimental apparatus

Fig. 2 – Image reconstruction procedure and nomenclature

system records this signal. At the end of each test, an application software is used to calculate both the average and the maximum variation of the rotational speed.

The employed infrared thermographic scanner is the AGEMA Thermovision 900. The field of view (which depends on the optics focal length and on the viewing distance) is scanned by the Hg-Cd-Te detector in the 8-12mm infrared band. Nominal sensitivity, expressed in terms of noise equivalent temperature difference, is $0.07°C$ when the scanned object is at ambient temperature. The scanner spatial resolution is 235 instantaneous fields of view per line at 50% slit response function.

The detection of the disk center position is clearly very important. In the present case, to facilitate its identification, an air jet is used. The jet, which impinges not far from the disk center, cools the disk surface creating, on account of the high response time of the disk, circular isotherms. By confronting a circular shape with the isotherms, it is possible to precisely detect the position of disk center in the thermal image.

In order to acquire an image of the surface temperature that is stationary with respect to the rotating disk the acquisition frequency of the thermographic system should be significantly higher of the rotational frequency. The used

thermographic system has a maximum acquisition frequency of only 15Hz and, clearly, this value is inadequate to follow the rotation of the disk. In order to acquire still (with respect to the rotating disk) thermal images of the surface temperature, the line scan facility of the IR camera is used so as to take temperature radial profiles.

As shown by the blue lines in Fig. 2 the thermographic system scans a horizontal line that is fixed in space. Due to the disk rotation each acquired line is displaced, relative to the disk surface, of an angle that is function of the rotating speed and of the acquisition frequency. Furthermore, due to the increase in absolute velocity moving towards the disk edge, the scanned line assumes a spiral profile on the disk surface (see lines 1 and 2 in figure). In order to create a thermal map that is stationary with respect to the rotating disk a numerical reconstruction is performed.

While, the local radius for each point of the scanned line is easily calculated from geometrical considerations, the polar coordinate is a function of time. By knowing the two polar coordinates it is possible to position each acquired temperature level in the thermal map. Even if, in the line scan mode, the used thermographic system has a maximum acquisition frequency of about 2.5 kHz, which could allow neglecting the spiral deformation of the acquired lines, this effect is taken into account while performing the reconstruction of the thermal image.

In order to reduce the noise a large number of radial profiles (about 15,000) are acquired during each test so that each point of the reconstructed image is, really, an average in time of the measured temperature levels.

In Fig. 2 is also shown the convention used for measuring the angle j (red lines). The local Reynolds number is defined as:

$$Re_r = \frac{w\, r^2}{n} \qquad (2)$$

where w is the angular speed, r the local radius and n the air kinematic viscosity. Instead, the
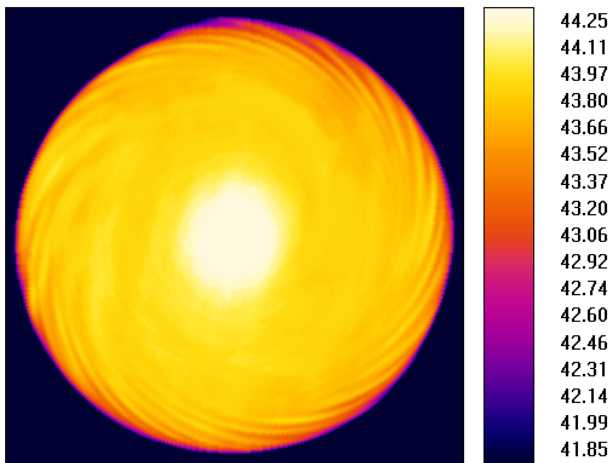
Fig. 3 – Disk thermal map for *Re* = 310,000

total Reynolds number *Re* is based on the disk external radius *R*.

3 Visualizations of the vortices

The thermal images are reconstructed both in the form of cartesian (*x* and *y* coordinates) and polar (*q* and *r* coordinates) maps. The former ones are used for visualization purposes while the latter ones for their post processing.

In order to understand the following thermal maps, it has to be noticed that, by neglecting the variations of the radiative heat flux over the disk surface and because of the constant imposed heat flux, to an increase of the convective heat transfer coefficient corresponds a decrease of the surface temperature and this explains the variations of wall temperature.

A typical example of a cartesian reconstructed image is shown in Fig. 3. The total Reynolds number is equal to 310,000, the disk is rotating in the clockwise direction and its diameter coincides with the side of the map. For this rotational regime, the flow should be laminar practically over the whole disk and, as expected from the theory, the convective heat transfer coefficient should be constant over the surface of the disk. Indeed the temperature over the disk surface is found to be constant apart from some variations towards the external part of the disk that should be attributed to the onset of vortices.

In order to understand the physical phenomenon let first analyze the effect of a single vortex by moving on the wall across it. The vortex takes fresh air from ambient and pushes it towards the surface of the disk producing, locally, a decrease of the surface temperature. Meanwhile, the impinging jet effect, induced by the vortex, increases at the same location the convective heat transfer coefficient and produces a further decrease of the local surface temperature. Afterwards, the fresh air flowing over surface of the disk increases its bulk temperature and, in the mean time, decreases the local convective heat transfer coefficient. Both these effects cause an increase of the surface temperature. Finally, the vortex expels the heated air towards the ambient and the process starts again.

The presence of various co-rotating vortices does not modify significantly this behavior and along circumferential lines, a quasi-sinusoidal varying convective heat transfer coefficient is expected.

Clearly, the temperature variations are proportional to the strength of the vortices and, as it is possible to see from the temperature scale on the right hand side of the map, in the present case, are very small (about 1K). The maps temperature range and mean level of Fig. 3, as well as those of the following ones, have been chosen in order to enhance the visualization of the vortices. This choice does not allow to see the rapid decrease of the temperature due to the transition to turbulent flow and the external part of the disk.

By moving towards the external part of the disk it is possible to see that some vortices have a tendency to split in two. The vortex splitting is the cause of the increase of the number of vortices for increasing local Reynolds number.

In Fig. 4 and 5 the surface temperature maps of the disk for a total Reynolds number equal to 450,000 and 560,000 respectively are shown. To an increase of the total Reynolds number corresponds an increase of the angular speed and, as a consequence, the displacement of the transition region towards the disk center so that the local transitional Reynolds number range remains practically constant. For this reason, as it is possible to see, a great part of the
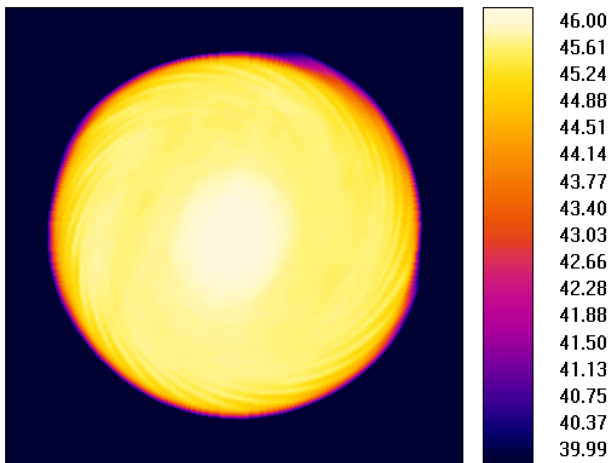
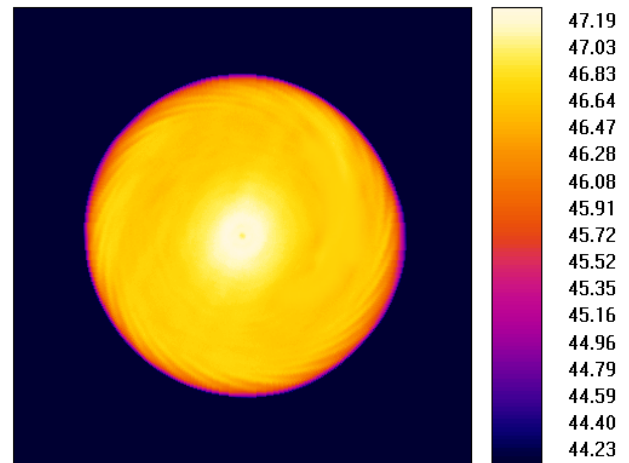Fig. 4 – Disk thermal map for *Re* = 450,000

Fig. 5 – Disk thermal map for *Re* = 560,000

disk surface is at low temperature and disappears in the maps.

Apart from a more regular behavior of the vortices over the disk, the temperature maps main features do not change significantly for increasing *Re*.

4 Numerical post processing

As already mentioned, the thermal maps are also reconstructed in the form of polar images; in Fig. 6 a typical example of such a reconstruction, for the same condition of Fig. 5, is shown. In particular, the vertical axis corresponds to the radius *r* while the horizontal one to the polar coordinate ***q***.

The use of this type of reconstruction enables to have temperature profiles, as a function of the polar coordinate ***q***, for various different local radii. An example of such a profile, relative to the dotted line in Fig. 6, is shown in Fig. 7a. Due to the very low temperature differences (about 0.5°*C*), induced by the vortices, the temperature profile appears quite noisy. Clearly, this noise has to be removed in order to simplify the numerical detection of the vortices.
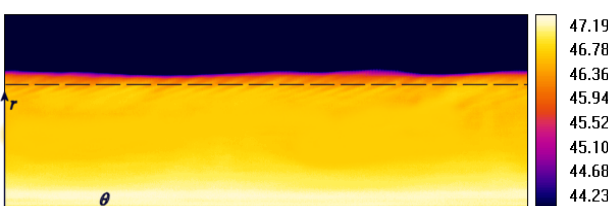

Fig. 6 – Polar reconstruction for *Re* = 560,000

The numerical method for the evaluation of the number of vortices is simply based on the detection of the number of pairs of successive maxima and minima. A typical example of the application of this method for the temperature profile of Fig. 7a is shown in Fig. 7b, where the temperature profile has been filtered with and ideal low pass filter with a cut off frequency that enables the detection of up to 50 vortices maximum. In the figure the numerically detected maxima and minima are reported with red circles.

In Fig. 7b by counting, the number of pairs of successive maxima and minima one can easily detect 25 vortices. The advantage of directly counting the vortices with respect to performing a spectral analysis is that with the latter method, it is possible only to measure the mean wavelength so that this method fails in the case of vortex splitting.

On the other hand, in the evaluation of the angle *j*, in order to increase the level of confidence, it is better to use an approach that is based on mean quantities. By making the cross correlation of two nearby temperature profiles it is possible to measure the local displacement of the temperature profiles along a radius. The cross-correlation coefficient *C* between the temperature profile, already shown in Fig. 7, and a nearby one is shown in Fig. 8. As it is possible to see, the cross correlation coefficient has a periodic behavior with a period that is function of the mean wavelength. By precisely detecting the position of the first right maximum
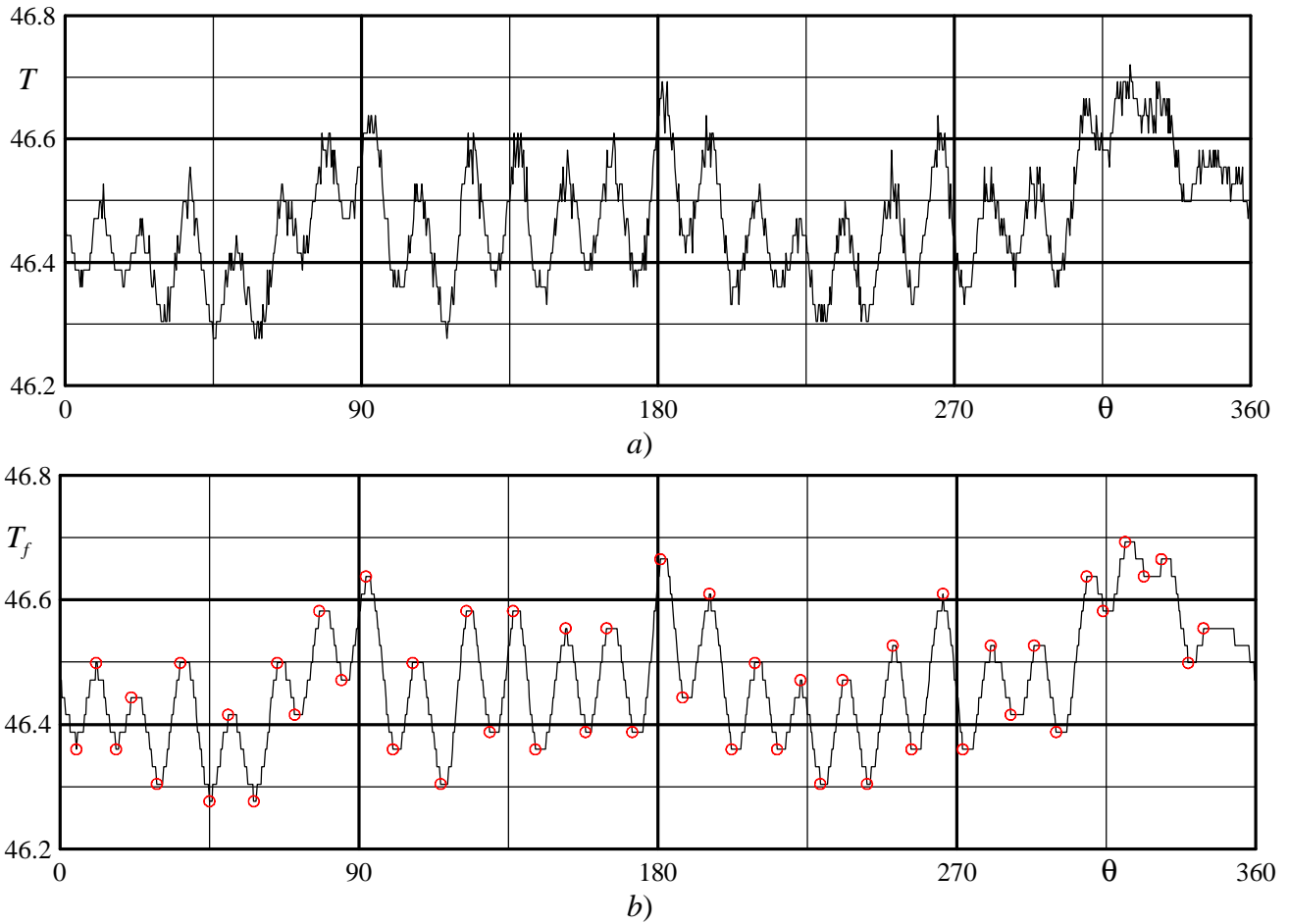
Fig. 7 –*a*) Raw temperature profile; *b*) Filtered temperature profile and location of local maxima and minima.

it is possible to evaluate the mean displacement. The good match between successive temperature profiles is testified by the relatively high (0.95) value of the first and absolute maximum. The decreasing value of the local maxima, for an increase of $\boldsymbol{q}$, is due to the non-perfect spacing between the vortices.

The following equation defines the angle $\boldsymbol{j}$:

$$tan\,\boldsymbol{j} = \frac{d\,ln\,r}{d\boldsymbol{q}} \qquad (3)$$

By discretizing this equation one obtains:

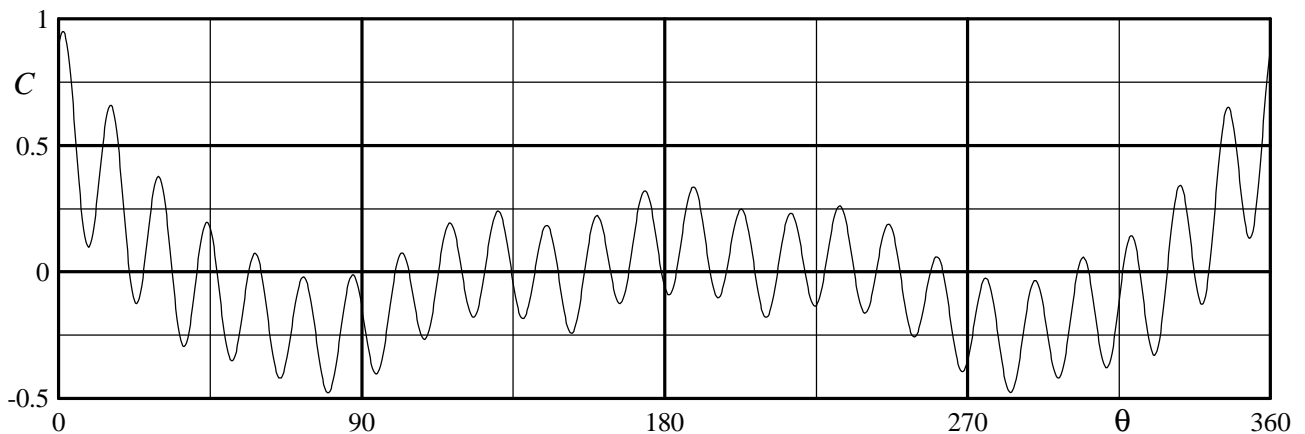$$\boldsymbol{j} = arctan\frac{ln\dfrac{r_1}{r_2}}{\Delta\boldsymbol{q}} \qquad (4)$$

Fig. 8 – Cross correlation of two successive temperature profiles.

In this equation Δq is the displacement of the first maximum from the origin; r_1 is the first local radius and r_2 the radius of the nearby temperature profile.

5 Quantitative results

The number of vortices N, counted with the method above explained, is plotted in Fig. 9 as a function of the local Reynolds number. In this figure about 80 different tests, performed by varying the angular velocity and the wall heat flux, are considered. The total number of point in the graph is over two thousands and this may explain the relatively high scatter of the experimental data.

For low values of Re_r the increase of N for increasing local Reynolds number is due to the vortex splitting already found by previous authors.

In the Re_r range from about 180,000 to about 240,000 the number of vortices remain

practically constant and goes from 23 to 26. These values are significantly smaller than those found by previous authors [6]. This could be ascribed to the different experimental technique. Really, the imposed heat wall heat flux creates a temperature gradient at the wall which, due to the dependence of viscosity from temperature, causes a viscosity gradient. The curvature of the velocity profile is in turn influenced by this viscosity gradient and the stability characteristics may therefore change significantly. No relevant correlation between the imposed heat flux and N is found.

For high local Reynolds number the decrease of the number of vortices may be ascribed to local burst transition to turbulence.

The spiral vortex angle is plotted, as a function of the local Reynolds number, in Fig. 10. In this case the Re_r interval is reduced because the above described numerical method fails for very small temperature differences, i.e. very small and very high local Reynolds
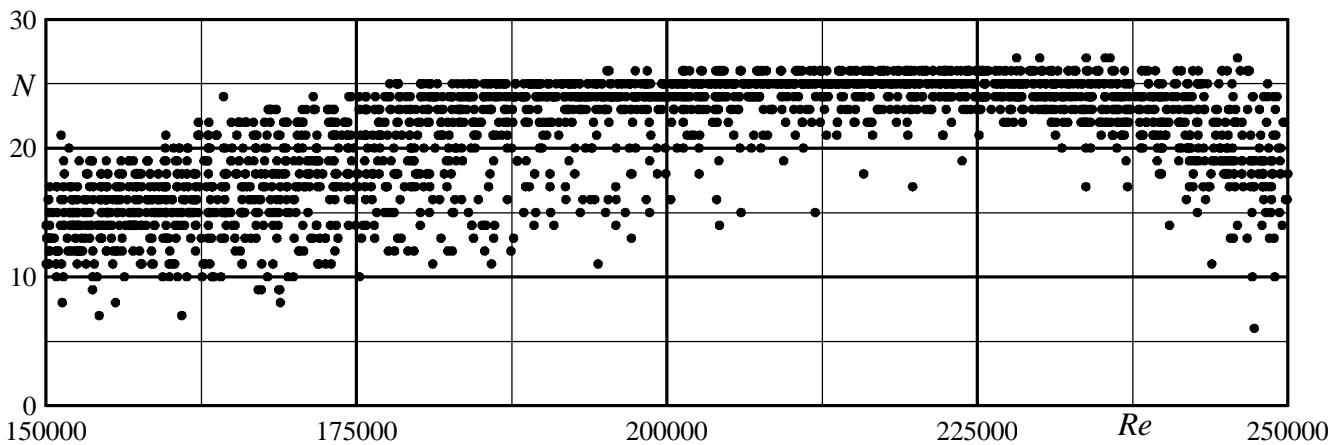

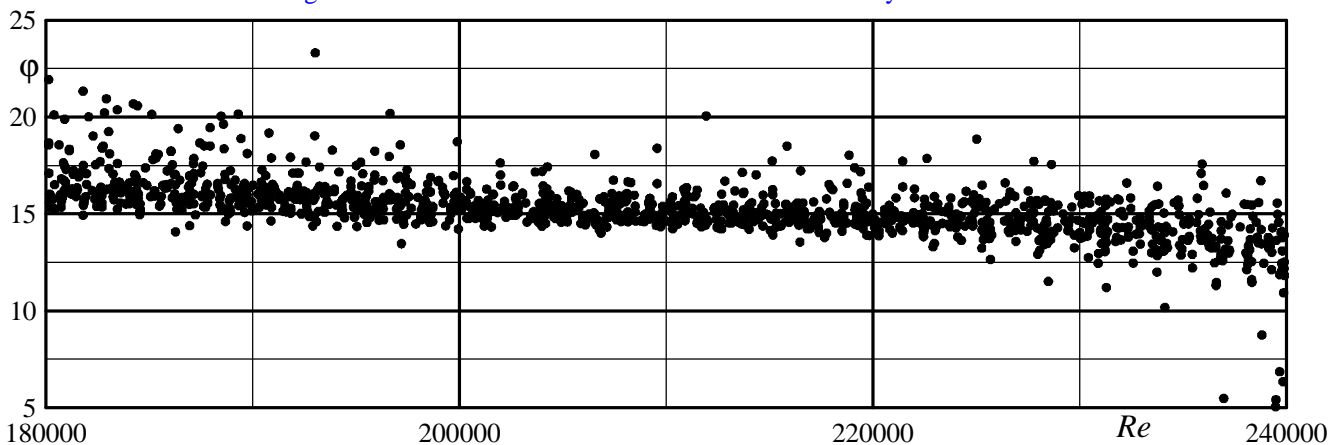Fig. 9 – Number of vortices as a function of the local Reynolds number.

Fig. 10 – Spiral vortex angle as a function of the local Reynolds number.

numbers.

The j mean value is about 15 degree and is in accordance with both the theoretical prediction and experimental data of Kobayashi et al. [6]. The clear tendency, to a decrease of j with an increase of the local Reynolds number is, as well, in harmony with the experimental data reported in Ref. [6]. Most probably, the imposed wall heat flux does not significantly influence the spiral vortex angle.

5 Conclusions

By using Infrared Thermography the spiral vortices that are present in the transitional regime of the flow on a disk rotating in still air are experimentally investigated

The detection of the vortices is achieved by uniformly heating the disk surface with a printed circuit board. The line scan facility of the thermographic system is used in order to reconstruct an image that is fixed to the rotating disk reference system.

Visualization of the vortices, in terms of temperature maps, show that, an increase of the local Reynolds number causes a movement of the vortices towards the disk center but does not alter significantly neither the vortices number nor the spiral vortex angle.

For low values of Re_r the increase of N for increasing local Reynolds number is due to the vortex splitting effect.

Due to the different thermal boundary condition, the average number of vortices that appears on the disk is significantly smaller than that already found by previous authors. On the other hand, the boundary condition does not seem to affect the mean value of the spiral vortex angle.

References

[1] Millsaps K. and Pohlhausen K. Heat Transfer by Laminar Flow from a Rotating Plate. *J. Aeronautical Science*, Vol. 19, pp. 120-126, 1952.

[2] Cobb E. C. and Saunders O. A. Heat Transfer from a Rotating Disk. *Proc. Royal Society*, Vol. 236, pp. 343-351, 1956.

[3] Northrop A. and Owen J. M. Heat Transfer Measurements in Rotating-disk Systems. Part 1: The Free Disk. *Int. J. Heat and Fluid Flow*, Vol. 9, No. 1, pp. 19-26, 1988.

[4] Cardone G., Astarita T. and Carlomagno G. M. Heat Transfer Measurements on a Rotating Disk. *Int. J. of Rotating Machinery*, Vol. 3, No. 1, pp. 1-9, 1997.

[5] von Kàrmàn Th.. Laminare und Turbulente Reibung, *ZAMM*, vol 1, pp. 233-252, 1921.

[6] Kobayashi R., Y. Kohama and Takamadate Ch. Spiral Vortices in Boundary Layer Transition Regime on a Rotating Disk, *Acta Mech.*, Vol. 35, pp. 71-82, 1980.

[7] Kohama Y. Study on Boundary Layer Transition of a Rotating Disk, *Acta Mech.*, Vol. 50, pp. 193-199, 1984.

[8] Malik M. R., Wilkinson S. P. and Orszag S. A. Instability and Transition in Rotating Disk Flow, *AIAA J.*, Vol. 19, pp. 1131-1138, 1981.

[9] Wilkinson S. P. and Malik M. R. Stability Experiment in the Flow over a Rotating Disk Flow, *AIAA J.*, Vol. 23, pp. 588-595, 1984.